

## Flow pattern maps of double emulsions transporting through bifurcation microchannels——Supplementary Information

Xiang Wang<sup>1</sup>, Chao Sun<sup>2</sup>, Shiyan Jia<sup>2</sup>, Yan Pang<sup>1,\*</sup>, Zhaomiao Liu<sup>1,\*</sup>

<sup>1</sup>*School of Mathematics, Statistics and Mechanics, Beijing University of Technology, Beijing 100124, China*

<sup>2</sup>*School of Mechanical & Energy Engineering, Beijing University of Technology, Beijing 100124, China*

\*Corresponding author: pangyan@bjut.edu.cn, lzm@bjut.edu.cn

### 1. Liquids

FC-40 was produced by 3M Electronics Markets Materials Division and repackaged by Shanghai Silver Tech Co., Ltd. Silicone oil PMX-200 (50 and 100 mPa s, neat) were purchased from Shanghai Aladdin Biochemical Technology Co., Ltd. PVA (brand: Alfa Aesar, 87-89% hydrolyzed) was purchased from Beijing InnoChem Science & Technology Co., Ltd. Sunflower oil (brand: Fulinmen) was purchased from Taobao.

The interfacial tension  $\gamma$  was measured by a platinum Wilhelmy plate (Model A201, Solon Tech., China) and the accuracy is 0.04 mN/m. Three measurements were carried out to obtain the interfacial tension and the average value with one decimal place was used. The dynamic viscosity  $\mu$  was measured using a rheometer (R/S-CPS Plus, Brookfield, USA) with a cone plate and the accuracy is 0.1 mPa s. The viscosities of the silicone oils were used as obtained while those of other liquids were measured at least three times to calculate the average values. For the measured results, the standard deviation is smaller than 0.1 mPa s, and therefore merely the average values are shown in Table 1.

## 2. Contacting angle

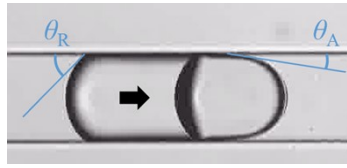


Fig. S1 Schematics of two contacting angles, i.e. the advancing angle  $\theta_A$  and the receding angle  $\theta_R$ . The solid arrow indicates the flow direction of the droplet. During movement, the advancing angle  $\theta_A$  is smaller than the receding angle  $\theta_R$  due to the shear stress. The two angles are smaller than  $90^\circ$ , indicating the hydrophilicity of the treated channel walls.

## 3. Daughter droplet size

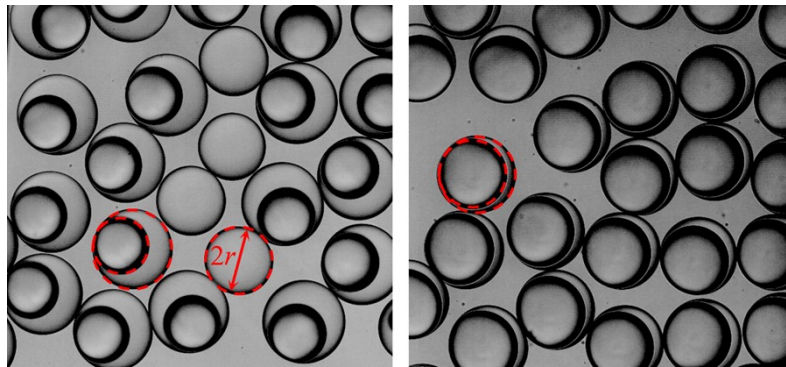


Fig. S2 Schematics of the daughter droplet radius. In the large collection chamber, the droplets are not deformed laterally and exhibit a circle profile in the top view, as indicated by the dashed circles. The droplet radii can be easily measured by the ImageJ software.

#### 4. Data fitting of the boundaries

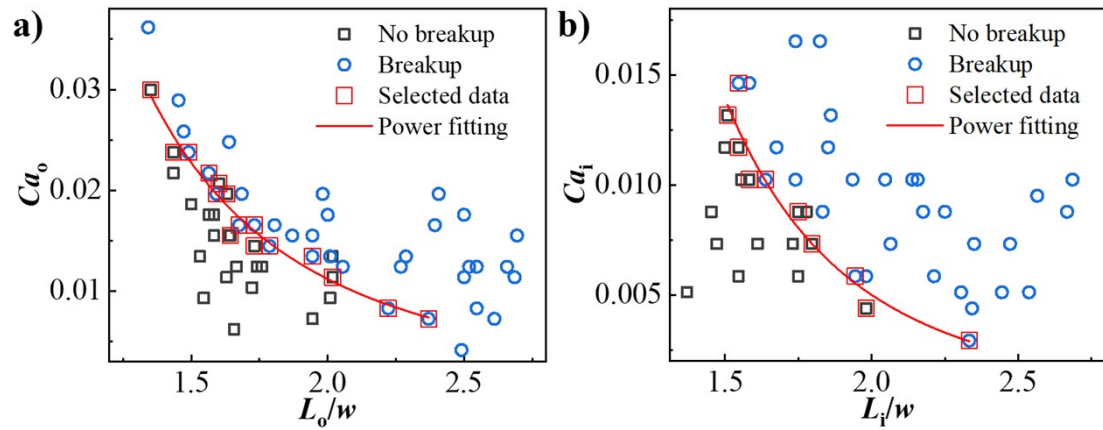


Fig. S3 Details of the power fitting results of the breakup boundaries in Fig. 8. To obtain the quantitative expression of the breakup boundary in the flow pattern map, the data points close to the boundary are used for fitting. The selected data points in a) and b) are highlighted by larger red boxes. The best fitting results via the power law relation  $y=ax^b$  are indicated by solid lines with fitting parameters: a)  $a=0.06188\pm 0.00424$ ,  $b=-2.46792\pm 0.14549$ ,  $R^2=0.96$ , b)  $a=0.05902\pm 0.01195$ ,  $b=-3.55996\pm 0.41874$ ,  $R^2=0.93$ . Note that the fitting results are transformed into  $L_0/w=\alpha Ca_0^b$  in the main manuscript which is the commonly-seen form.